JOURNAL OF MATERIALS SCIENCE 28 (1993) 4341–4346

# Viscoelastic effects in testing of an $Al_2O_3$ ceramic containing a glassy phase

H. PETERLIK
*Max-Planck-Institut für Metallforschung, Institut für Werkstoffwissenschaft, Seestraße 92, D-7000 Stuttgart, Germany*

K. KROMP
*Institut für Festkörperphysik, University of Vienna, Boltzmanngasse 5, A-1090 Vienna, Austria*

An alumina with 3 wt% glassy phase was tested at different loading rates at two temperatures (900 and 1000 °C). It was found that an increase in fracture toughness was accompanied by a decrease of the bending strength at the same loading rates. A model is given, which describes the experimental results by linear viscoelasticity of the second phase. Whereas the bulk properties are mainly due to the alumina grains and, therefore, remain nearly unchanged, the crack growth and the fracture behaviour in the intergranular regions is dominated by the viscosity of the glassy phase. This leads to a non-unique value of $K_{Ic}$, which is dependent on the temperature and the loading rate.

## 1. Introduction

The strength behaviour of ceramics especially under high-temperature conditions is of particular interest. In contrast to the subcritical crack growth at room temperature, which is mainly due to the corrosive influence of the environment [1, 2] (usually the partial pressure of water vapour), the crack growth at high temperatures is a consequence of diffusion, creep and viscoelasticity. Because there are different mechanisms which control the mechanical behaviour in the different temperature regions, it is difficult to define general material properties such as fracture toughness, bending or tensile strength. Some studies on the mechanical behaviour of different ceramics with a glassy phase have shown that the fracture toughness is not constant at high temperatures [3, 4], yet the problem is not well understood. In this work a model, which shows the influence of the sintering additives on the mechanical behaviour of ceramics at elevated temperatures, is proposed. Alumina was chosen as a model material, because it can be sintered with and without glassy phase. Thus one can compare results of alumina with glassy phase with measurements of the pure material to determine the influence of the viscous phase [3] or the influence of different loading conditions [5, 6].

## 2. Experimental procedure

The material tested was an alumina with 3 wt% glassy phase. The second phase was mainly localized in the grain boundaries and the triple points, and its composition was determined by energy dispersive spectroscopy (EDS) and can be seen in Table I. The amount of alumina in the glassy phase is questionable, because the surrounding alumina grains may influence the measurement. The medium grain size was 10 μm, the largest grains were about 70 μm. Table II shows further material parameters [4].

TABLE I Composition of the glassy phase

| | at % | wt % | Formula | Comp. % |
|---|---|---|---|---|
| Si | 23.1 | 31.8 | $SiO_2$ | 68.1 |
| Al | 9.0 | 11.9 | $Al_2O_3$ | 22.4 |
| Ca | 1.4 | 2.8 | CaO | 3.9 |
| Mg | 1.9 | 2.2 | MgO | 3.7 |
| Na | 1.3 | 1.4 | $Na_2O$ | 1.9 |

TABLE II Some material properties of the tested alumina

| | | |
|---|---|---|
| Density | 3760 | $kg\,m^{-3}$ |
| Grain size | ~ 10 | μm |
| Young's modulus (RT) | 342 | GPa |
| $K_{Ic}$ (RT) | $3.8 \pm 0.6$ | $MPa\,m^{1/2}$ |

The material was tested in a hydraulic testing apparatus containing a four-point bending device with a fixed roller system at a span of 20/40 mm, described in detail elsewhere [7]. The size of the tested specimens was $3 \times 4 \times 45\ mm^3$ according to DIN-standard 51110. High temperature was achieved by induction heating, and all tests were performed in air. For $K_{Ic}$ tests, the specimens were cut with a diamond saw equipped with a 50 μm blade in order to achieve a notch width below 100 μm. The notch depth to specimen width ratio was chosen $0.2 < a/W < 0.3$, according to DIN proposal 51109.

## 3. Results

Fig. 1 shows the dependence of fracture toughness, $K_{Ic}$, and bending strength, $\sigma_B$, on the loading rate, $\dot{\sigma}$,

0022–2461 

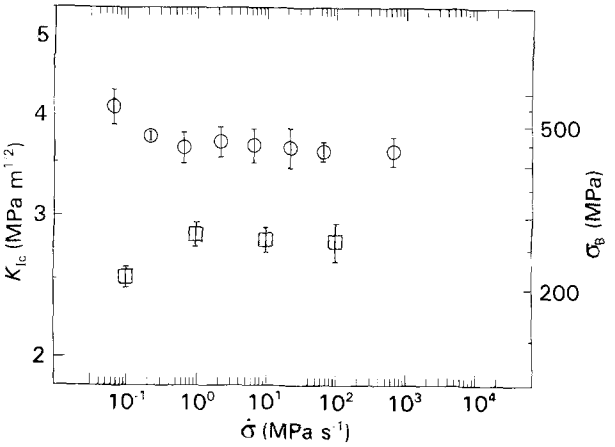


*Figure 1* (○) Fracture toughness, $K_{Ic}$, and (□) bending strength, $\sigma_B$, at 900 °C versus loading rate, log $\dot{\sigma}$.

at 900 °C. It is well known that the bending strength for four-point bending is given by

$$\sigma_B = \frac{3Fe}{BW^2} \tag{1a}$$

and $K_{Ic}$ by

$$K_{Ic} = \frac{3Fe}{BW^2} Y(\pi a)^{1/2} \tag{1b}$$

where $F$ is the fracture force, $B$ and $W$ the breadth and width of the specimen, respectively, and $e$ the leaver arm. The experiments were performed at different constant loading rates, $\dot{\sigma}$ and $\dot{K}$. If one differentiates Equation 1b with respect to the time, one can see that

$$\dot{\sigma} = \frac{\dot{K}}{Y(\pi a)^{1/2}} \tag{2}$$

According to this equation, it is possible to plot bending strength values as well as fracture toughness values in the same diagram (see Fig. 1). Each point represents the mean value of five tests, the bars show the mean deviation.

The most interesting point to be seen in this diagram is that starting from high loading rates from the right-hand side of the diagram, the bending strength decreases, whereas the $K_{Ic}$ values start to increase at the same loading rate. For the low and high loading rates, the fracture appearance is different (the scanning electron micrographs are taken from the fracture surfaces of the $K_{Ic}$-tested specimens): there is mainly intercrystalline fracture at the lowest loading rate of $\dot{K} = 0.003$ MPa m$^{1/2}$ s$^{-1}$ (Fig. 2a), with the glassy phase at the grain boundaries, whereas for a loading rate of $\dot{K} = 300$ MPa m$^{1/2}$ s$^{-1}$, fracture is transcrystalline (Fig. 2b) and no glassy phase can be identified.

At the higher temperature of 1000 °C, one can see that the loading rate, at which the bending strength starts to decrease, moved to a significant higher level (Fig. 3), from which one can conclude that this effect may be a consequence of viscosity. The $K_{Ic}$ values again start to increase at the same loading rate, then they go through a maximum and turn out to have the same value for the lowest as well as for the highest loading rates (read from right to left in Fig. 3). The scanning electron micrographs show intercrystalline fracture for the low loading rate of

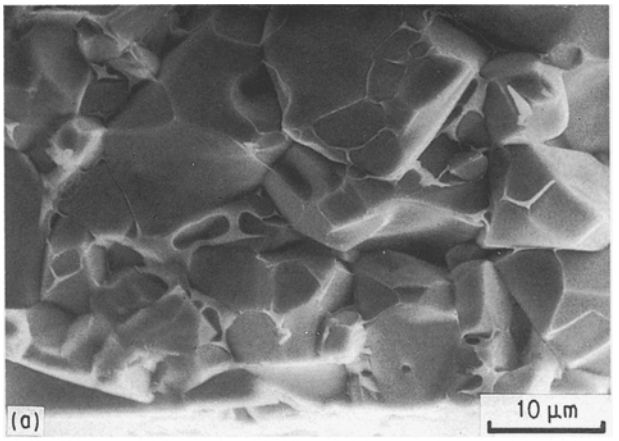


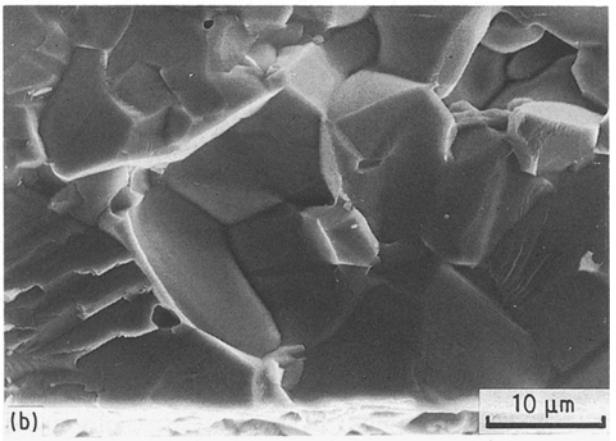


*Figure 2* Scanning electron micrographs at (a) the lowest loading rate of $\dot{K} = 0.003$ MPa m$^{1/2}$ s$^{-1}$, $\sim \dot{\sigma} = 0.03$ MPa s$^{-1}$ and (b) the high loading rate of $\dot{K} = 300$ MPa m$^{1/2}$ s$^{-1}$, $\sim \dot{\sigma} = 3000$ MPa s$^{-1}$, at 900 °C.

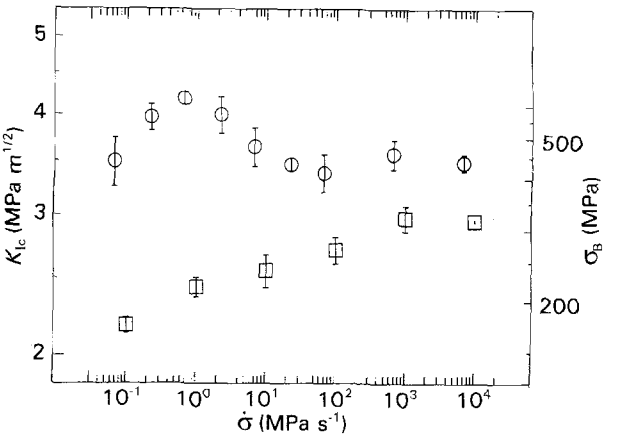


*Figure 3* (○) Fracture toughness, $K_{Ic}$ and (□) bending strength, $\sigma_B$, at 1000 °C versus loading rate, log $\dot{\sigma}$.

$\dot{K} = 0.003$ MPa m$^{1/2}$ s$^{-1}$ (Fig. 4a). The glassy phase is clearly visible as "fingers" at the grain boundaries. For a loading rate of $\dot{K} = 0.03$ MPa m$^{1/2}$ s$^{-1}$ (Fig. 4b), the location where the maximum in $K_{Ic}$ appears, one can see a mixed-mode fracture, which resembles the micrographs for the lower loading rate at 900 °C, and only for very high loading rates of $\dot{K} = 300$ MPa m$^{1/2}$ s$^{-1}$ (Fig. 4c) is fracture again transcrystalline. These scanning electron micrographs

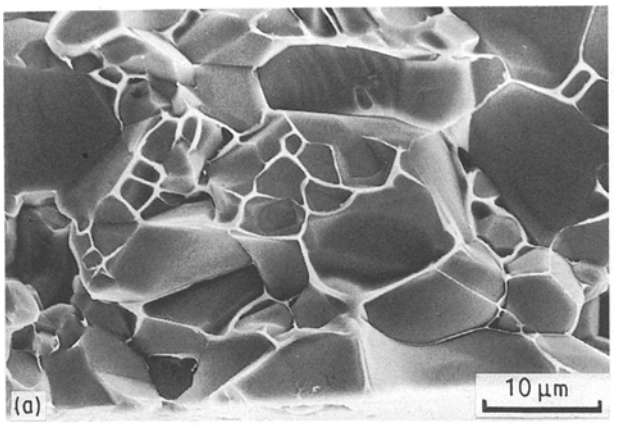


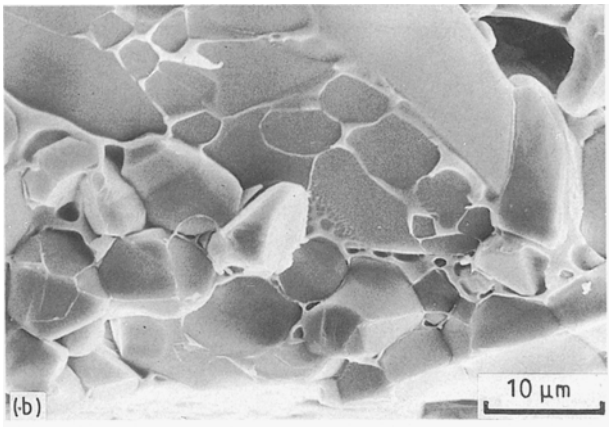


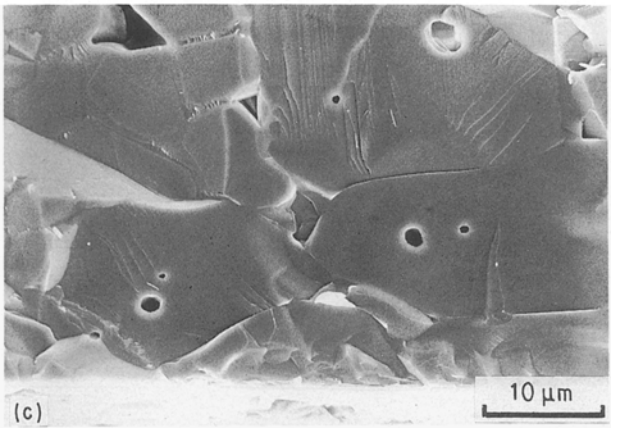


*Figure 4* Scanning electron micrographs at (a) the lowest loading rate of $\dot{K} = 0.003\ \mathrm{MPa\,m^{1/2}\,s^{-1}}$, $\sim \dot{\sigma} = 0.03\ \mathrm{MPa\,s^{-1}}$, (b) the loading rate of $\dot{K} = 0.03\ \mathrm{MPa\,m^{1/2}\,s^{-1}}$, $\sim \dot{\sigma} = 0.3\ \mathrm{MPa\,s^{-1}}$ near the maximum of $K_{Ic}$, and (c) the high loading rate of $\dot{K} = 300\ \mathrm{MPa\,m^{1/2}\,s^{-1}}$, $\sim \dot{\sigma} = 3000\ \mathrm{MPa\,s^{-1}}$, all at 1000 °C.

clearly show the influence of the glassy phase on the crack extension.

## 4. Discussion

From the experimental data it can be stated that the second phase begins to "soften" at a certain point, which is dependent on the temperature (and thus on the viscosity of the glassy phase) as well as on the loading rate. This critical point in the loading rate corresponds to a certain relaxation time $\tau(\dot{\sigma}, T)$. At loading rates lower than the loading rate, which allows firstly a relaxation time $\tau$, the "softening" of the second phase promotes the separation of grains and therefore a subcritical crack growth, which leads to a decrease in the bending strength. On the other hand, the "softening" of the viscous phase is responsible for a stress relaxation at the crack tip in the same regime of loading rates. This, however, leads to an increase of $K_{Ic}$, because now the effective stress at the crack tip decreases. An increase in crack length due to subcritical crack growth has no effect on $K_{Ic}$, because it is small in comparison to the depth of the notch.

The relaxation behaviour can be described by a model of springs and dashpots. If one assumes a linear viscoelastic behaviour for one Maxwell element, the total strain rate is

$$\dot{\varepsilon}_{tot} = \frac{\dot{\sigma}}{E} + \frac{\sigma}{\eta} \qquad (3)$$

where $\eta$ is the viscosity of the dashpot and $E$ the Young's modulus of the spring. Equation 3 can be solved for the spring and the dashpot, respectively.

Then the strain of each element is given by

$$\varepsilon_s = \dot{\varepsilon}_{tot}\, t\, e^{-\frac{t}{\tau}}$$
$$\varepsilon_d = \dot{\varepsilon}_{tot}\, t\,(1 - e^{-\frac{t}{\tau}}) \qquad (4)$$

where the subscript s denotes the spring, and d the dashpot.

$$\tau = \eta/E \qquad (5)$$

is the relaxation time. If the stress has time to relax, there exists a "process region", into which the stress can expand. In this region there is a number of grain boundaries with glassy phase of different thickness at its triple points. The mechanical behaviour of these viscous parts is now modelled by a Gaussian distribution of a number, $N$, of dashpots with different viscosities and thus by different relaxation times around $\tau_{max}$, according to Equation 5, see Fig. 5

$$\tau_i = \tau_{max}\, e^{-h\left(i-\frac{N}{2}\right)^2} \qquad i = 1\text{–}N \qquad (6)$$

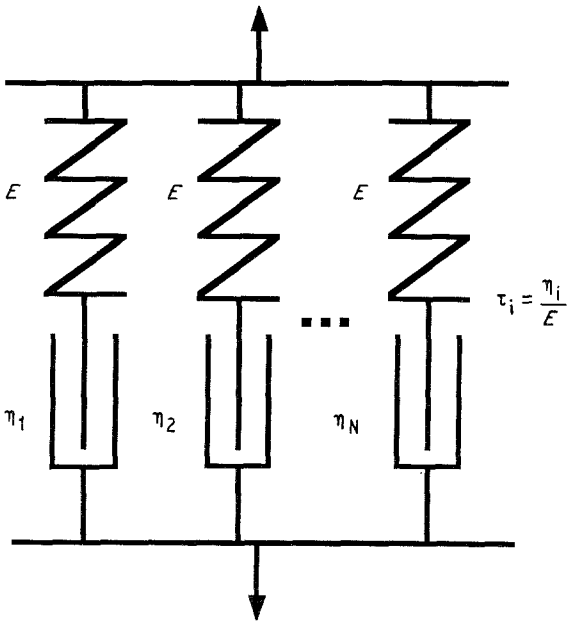


*Figure 5* Model of the system of Maxwell-elements, which take up the strain at the crack tip.

with $h$ the half width of the distribution. As a consequence, one has to write Equation 4 for different elements $i$

$$\varepsilon_{s_i} = \dot{\varepsilon}_{tot} t e^{-\frac{t}{\tau_i}} \quad (7a)$$

$$\varepsilon_{d_i} = \dot{\varepsilon}_{tot} t(1 - e^{-\frac{t}{\tau_i}}) \quad (7b)$$

with $\tau_i$ the different relaxation times characteristic for each element. The total strain which the specimen can sustain, is

$$\varepsilon_{tot} = \sum_{i=1}^{N} (\varepsilon_{s_i} + \varepsilon_{d_i}) \quad (8)$$

where $N$ is the number of the elements. Now, there is no difference in time-developing the strain or in time-developing the $K$-factor under the rough presumption that the bulk of the specimen still behaves in a linear elastic way. The only assumption is that the $K$-factor behaves in a time-dependent manner at the crack tip, in the same way as the strain defined above. Then one can write Equations 7a and b for the time-development of the $K$-factors of spring and dashpot

$$K_{s_i} = \dot{K} t e^{-\frac{t}{\tau_i}} \quad (9a)$$

$$K_{d_i} = \dot{K} t(1 - e^{-\frac{t}{\tau_i}}) \quad (9b)$$

One can assume that for very high loading rates the material is brittle and the mechanical behaviour is dominated by the springs. Therefore, the maximum of the $K$-factor for the springs, which is $K_{Ic_s}$, can be taken from the experiments at very high loading rates. For very low loading rates the viscous phase has no influence, the hard alumina grains are in direct contact with each other and behave in a brittle manner as is the case for the very high loading rates. Under these circumstances, the material can be classified as porous, therefore $K_{Ic}$ for low loading rates is expected to be less or equal to the $K_{Ic}$ value for very high loading rates. For that reason the value from the experiments with the lowest loading rates is taken for the maximum of the $K$-factors for the dashpots, $K_{Ic_d}$, if no experimental values are available, which exhibit that $K_{Ic}$ is lower for the low loading rates. The measurements at 1000 °C, presented in Fig. 3, show that $K_{Ic}(\dot{K}_{high}) \simeq K_{Ic}(\dot{K}_{low})$. For 900 °C the lowest loading rates are not extended to this regime (Fig. 1). Nevertheless, former experiments in three-point bending [3] show the same feature at 900 °C

$$K_{Ic_s} = K_{Ic}(\dot{K}_{high}) \quad (10a)$$

$$K_{Ic_d} = K_{Ic}(\dot{K}_{low}) \quad (10b)$$

$$K_{Ic_s} = K_{Ic}(\dot{K}_{high}) \simeq K_{Ic}(\dot{K}_{low}) = K_{Ic_d} \quad (10c)$$

In the intermediate regime it is possible for the viscous phase to relax at the crack tip. This corresponds to the fact that in the mathematical model, springs as well as dashpots take a part of the strain. The operating $K$ is then

$$K_{tot} = \sum_{i=1}^{N} (K_{s_i} + K_{d_i}) \quad (11)$$

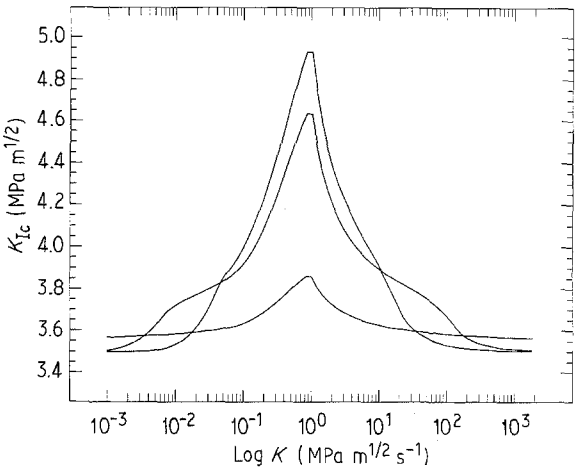


*Figure 6* Dependence of the computations on the distribution of the relaxation times for $h = 10^{-4}$, $10^{-3}$ and $10^{-2}$ in Equation 6.

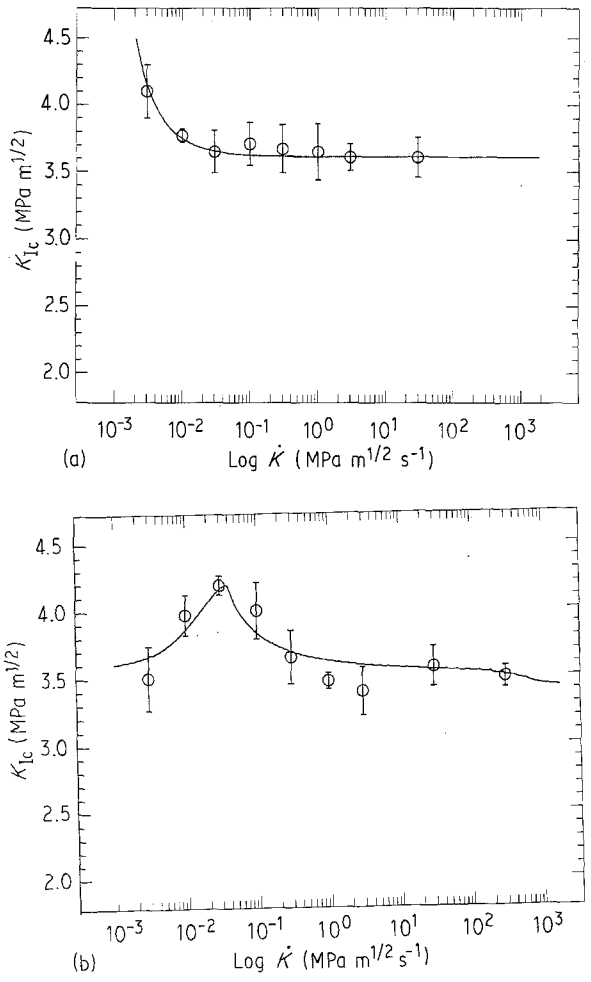


*Figure 7* Calculations for the models (a) with $\tau_{max} = 10000$ s and $h = 0.0001$ at 900 °C, and (b) with $\tau_{max} = 250$ s and $h = 0.004$ at 1000 °C.

The time-development is computed numerically and Equation 11 is stopped, if either the boundary condition for the spring $K_{s_i} = K_{Ic_s}$ or for the dashpot $K_{d_i} = K_{Ic_d}$, see Equations 10a–c, is reached. Then for a given loading rate, $K_{Ic} = K_{Ic}(t, \tau)$.

By this, one has two parameters, which can be varied to minimize the deviation of the calculated

$K_{Ic}$ from the measured values. First, the main parameter is $\tau_{max}$, which is responsible for the maximum of $K_{Ic}$. The second parameter is the half-width, $h$, of the Gaussian distribution and corresponds to the width of the distribution of the increased $K_{Ic}$ values. In fact, these two parameters are not independent: if one has a very small distribution, the peak in the $K_{Ic}$ value is high, whereas for flat distributions, which range over several decades, the peak is not very distinct (see Fig. 6). Thus, the result is rather unique and simple. In contrast to other models, which try to describe viscous effects, this model needs essentially only one parameter, the relaxation time (or thus the viscosity), whereas former approaches are based on a number of assumptions, which can hardly be determined, e.g. [8].

The minimum of the deviation from the experimental values is found by varying $\tau_{max}$ and $h$ simultaneously. The results are the fits in Fig. 7a and b with $\tau_{max} = 10\,000$ s for 900 °C. Because only one slope could be used for the fit in Fig. 7a, this value is an estimation, but, as mentioned before, the low loading rates could not be extended to the maximum with the hydraulic test equipment. $\tau_{max}$ changes to 250 s for 1000 °C. The curves are not smooth, because we restricted ourselves to 100 Maxwell-elements and did not compute a dense network in order to keep the computing time reasonably low.

## 5. Outlook

From the first parameter $\tau_{max} = \eta_{max}/E$, the mean viscosity, $\eta_{max}$, can be calculated. The real viscosity cannot be determined by this method, because $E$, the Young's modulus of the glassy phase, is not known, but it should be possible for the manufacturer to measure it. In our experiment only the relative viscosity of the second phase at 900 and 1000 °C can be determined. The simplest approach is to choose an Arrhenius equation for the viscosities, e.g.

$$\ln \frac{\eta_1}{\eta_0} = c\left(\frac{1}{T_1} - \frac{1}{T_0}\right) \tag{12}$$

In the literature, an increase in $K_{Ic}$ was also found, when the experiments were performed only at one loading rate, but for different temperatures [9]. From Equation 12 we obtain

$$\ln \eta - \frac{c}{T} = \text{constant} \tag{13}$$

With $\eta = \tau/E$ and $\tau_{max} \propto \dot{K}^{-1}$, which can be obtained by time-developing Equation 9 and checking the results for different $\tau$, we find

$$\ln \dot{K} + \frac{c_1}{T} = \text{constant} \tag{14}$$

Thus, we can conclude

$$K_{Ic}(\dot{K}, T) = F\left(\ln \dot{K} + \frac{c_1}{T}\right) \tag{15}$$

From the measurements at 900 and 1000 °C the parameters $c_1$ and the constant in Equation 14 can be determined as $c_1 = 22\,050$ K and the constant = 15.6. From this, we obtain Fig. 8. Here the peaks at the lower temperatures are drawn higher according to the fit in Fig. 7a, because it is reasonable to assume that the "process region" is smaller, if the viscosity of the second phase is higher. This is in accordance with $K_{Ic}$ measurements by Kromp and Pabst [3]. If we take this effect into account, the results in Fig. 8 are reached. Of course, the decrease in the maximum of the peak of the $K_{Ic}$ is an estimated value.

This estimation, however, is supported by the results in three-point bending with different spans in a crosshead speed-controlled [3] and in a displacement-controlled experiment [4]. Despite the different loading conditions, these results show principally the same behaviour, with the only difference being that the maximum appears at a different loading rate than for four-point bending. Fig. 9a shows these values and the previous results [3] at 900 °C, and in Fig. 9b the values of $K_{Ic}$ are shown for 1000 °C. The difference can be qualitatively explained by the fact that in four-point bending the region around the notch is loaded with a stress at a constant level. For three-point bending, however, the stress around the notch decreases with the distance from the notch, therefore the loaded volume is much smaller. Therefore, relaxation takes less time, and thus the maximum of the $K_{Ic}$ values is shifted to higher loading rates. This effect is more pronounced for the lower temperature, because of the higher viscosity of the glassy phase at the lower temperature. The ratio of the relaxation times of three-point to four-point bending is therefore higher for 900 °C than for 1000 °C.

From these experimental results one can calculate the dependence of $K_{Ic}$ on temperature and loading rate for three-point bending in the same way as was shown for four-point bending. The results are presented in Fig. 10, with $c_1 = 14\,250$ K and the constant = 12.1 in Equation 15.

As a consequence, the loading rate and also the mode of testing must be taken into account. The

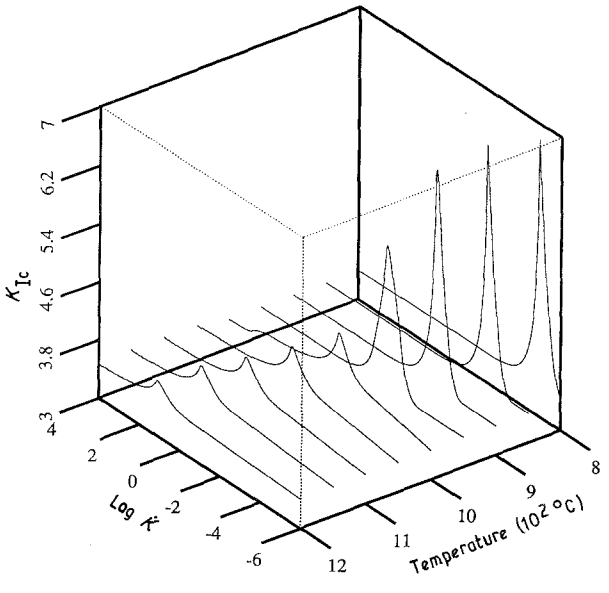


*Figure 8* Dependence of $K_{Ic}$ values of temperature and loading rate in four-point bending.

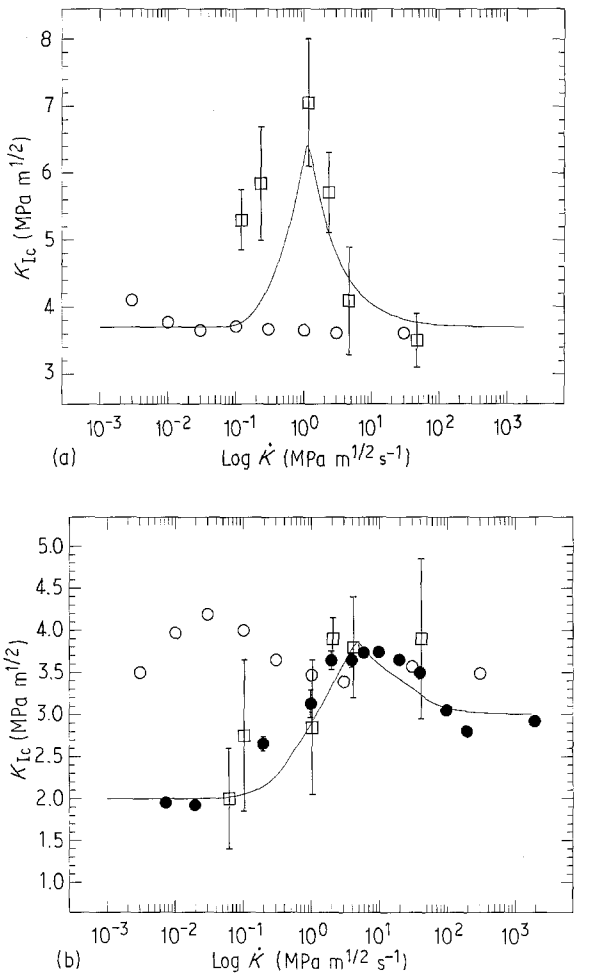


*Figure 9* (a) Values of $K_{Ic}$ at 900 °C in (○) four-point-bending and (□) 3-point-bending, from [3]. (b) Values of $K_{Ic}$ at 1000 °C in (○) four-point-bending and (□, ●) three-point bending (□ [3], (●) [4]).

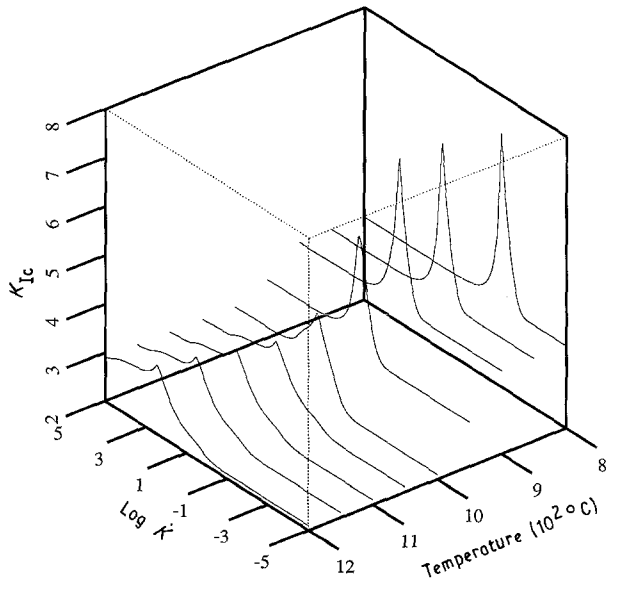


*Figure 10* Dependence of $K_{Ic}$ values on temperature and loading rate in three-point bending.

intention of this study, however, was not to give a complete description of the material $Al_2O_3$ with glassy phase, which would involve too great an experimental expense. Figs 8 and 10 should show the principal mechanical behaviour of ceramics with a second phase at high temperatures. According to this, it is our opinion that there exists no unique $K_{Ic}$ value at high temperatures for ceramics with glassy sintering additives. Even if tests are carried out at the same temperatures and at the same loading rates, it is not possible to compare the results, because one could be looking at a point near the peak in the case of one material and far from the peak in the case of another one, which is due to the different viscosities of their second phases. Only by measurements at two temperatures at least, and different loading rates or at two loading rates and different temperatures one can describe the mechanical behaviour according to the model presented. In practice, however, this would lead to high costs for the material and the experimental tests. On the other hand, materials with glassy phase will rarely find an application at temperatures where the glassy phase is fluid. Experiments should therefore be carried out at high loading rates and moderate temperatures, where the definition of $K_{Ic}$ as a material constant still holds.

## Acknowledgement

This work was supported by the Deutsche Forschungsgemeinschaft, Projekt Kr 970/3-2.

## References

1. W. PICHL, PhD thesis, University of Vienna (1986) pp. 70–9.
2. S. M. WIEDERHORN, S. W. FREIMAN, E. R. FULLER and C. J. SIMMONS, *J. Mater. Sci.* **17** (1982) 3460.
3. K. KROMP and R. F. PABST, *Metal Sci.* **3** (1981) 125.
4. T. HAUG, PhD thesis, University of Stuttgart (1985) pp. 74–86.
5. S. LAUF, V. GEROLD and R. F. PABST, in "Proceedings of the 4th International Conference on Fatigue and Fatigue Threshold", Vol. 2, Honolulu, Hawai 1990, edited by H. Kitagawa and T. Tanaka (MCEP, Birmingham, UK, 1990) p. 775.
6. C. L. LIN and D. F. SOCIE, *J. Amer. Ceram. Soc.* **74** (1991) 1511.
7. C. RIEF and K. KROMP, *Int. J. High Technol. Ceram.* **4** (1988) 301.
8. T. HAUG, A. C. BORNHAUSER, H. G. SCHMID, V. GEROLD and R. F. PABST, in "Proceedings of the 2nd International Conference on Creep and Fracture of Engineering Materials and Structures—Part I", Swansea 1984 (Pineridge Press, Swansea, UK, 1984) p. 473.
9. D. MUNZ, G. HIMSOLT and J. ESCHWEILER, "Fracture Mechanics Methods of Ceramics, Rocks, and Concrete", ASTM STP 745 (American Society for Testing and Materials, Philadelphia, PA, 1981) p. 69.

*Received 2 January*
*and accepted 2 September 1992*